

Reflection and Relay Dual-Functional RIS Assisted MU-MISO Systems

Yanan Ma[†], Rang Liu[†], Yang Liu[†], Ming Li[†], and Qian Liu[‡]

[†]School of Information and Communication Engineering

Dalian University of Technology, Dalian, Liaoning 116024, China

E-mail: {mayanan, liurang}@mail.dlut.edu.cn, {yangliu_613, mli}@dlut.edu.cn

[‡] School of Computer Science and Technology

Dalian University of Technology, Dalian, Liaoning 116024, China

E-mail: {qianliu}@dlut.edu.cn

Abstract—Reconfigurable intelligent surfaces (RISs) have been deemed as one of potential components of future wireless communication systems because they can adaptively manipulate the wireless propagation environment with low-cost passive devices. However, due to double fading effect, the passive RIS can offer sufficient signal strength only when receivers are nearby and located at the same side as the incident signals. Moreover, RIS cannot provide service coverage for the users at the back side of it. In this paper we introduce a novel reflection and relay dual-functional RIS architecture, which can simultaneously realize passive reflection and active relay functionalities to enhance the coverage. The problem of joint transmit beamforming and dual-functional RIS design is investigated to maximize the achievable sum-rate of a multiuser multiple-input single-output (MU-MISO) system. Based on fractional programming (FP) theory and majorization-minimization (MM) technique, we propose an efficient iterative transmit beamforming and RIS design algorithm. Simulation results demonstrate the superiority of the introduced dual-functional RIS architecture and the effectiveness of the proposed algorithm.

Index Terms—Reconfigurable intelligent surfaces, beamforming, relay, fractional programming (FP), majorization-minimization (MM).

I. INTRODUCTION

Reconfigurable intelligent surfaces (RISs) have been proposed as a promising technology for future wireless communication systems and extensively investigated in recent research works [1], [2]. Specifically, a RIS is an array composed of massive passive elements, which are connected to a controller. It can construct favorable wireless propagation environment between transmitters and receivers by changing the phase-shift of the reflected electromagnetic (EM) waves which impinge on the surface. Considering the low cost and low power consumption features, RISs have many promising applications in wireless systems for capacity optimization, secure transmission, enhancing energy/spectrum efficiency [3]-[5], etc.

However, due to “double fading” effect (i.e., the equivalent path loss of the transmitter-RIS-receiver link is the product of the path losses of the transmitter-RIS link and RIS-receiver link, which is usually an order of magnitude larger than that of the direct link), RIS should be deployed close to either the base station (BS) or users to effectively improve communication

performance [6]. Moreover, the reflective RIS property of restricts the service coverage to only one side of the surface and the users at the back of RIS cannot be served. Besides, recent studies showed that RISs can be easily outperformed by conventional full-duplex (FD) amplify-and-forward (AF) relay unless very large RISs are employed [7], [8]. However, very large number of reflecting elements will lead to high training overhead for channel estimation. Consequently, the control of RIS will also become more difficult [9]. Therefore, it is not very practical to place the RISs which can only passively reflect the incident signals to enhance the wireless communication.

Recently, in order to conquer the double fading effect and reduce the number of required reconfigurable elements, some proposals to improve RIS have been raised and attracted a lot of interest. In [10], the authors for the first time proposed a novel relay-aided RIS architecture consisting of two RIS surfaces connected via a full-duplex relay. This architecture can achieve the same performance with conventional RIS while only requiring much fewer reconfigurable elements. However, they only consider single-input single-output (SISO) system and derive the theoretical upper bound of achievable rate. The designs of BS beamforming and RIS reflection have not been well investigated. A further question is that the first RIS is only adjusted to reflect the signal towards relay and cannot simultaneously serve the users around it. In [11], the authors proposed a semi-active RIS-aided architecture which means that the RIS can not only passively reflect the signal, but also actively amplify it at the same time. However, the practical implementation of this hybrid-RIS remains an open problem, while it needs expensive radio frequency (RF) chains.

To overcome the double fading effect, enhance the coverage and reduce hardware complexity, in this paper we propose a novel reflection and relay dual-functional RIS architecture based on uniting two RISs back-to-back with an amplifier. The dual-functional RIS architecture can simultaneously realize passive reflection and active relay functionalities to enhance the coverage and the quality of service (QoS). Particularly, one RIS passively adjusts its phase shifters to serve the users close to and at the same side as this RIS. Meanwhile, the signal is amplified and transmitted by the other RIS to serve the users

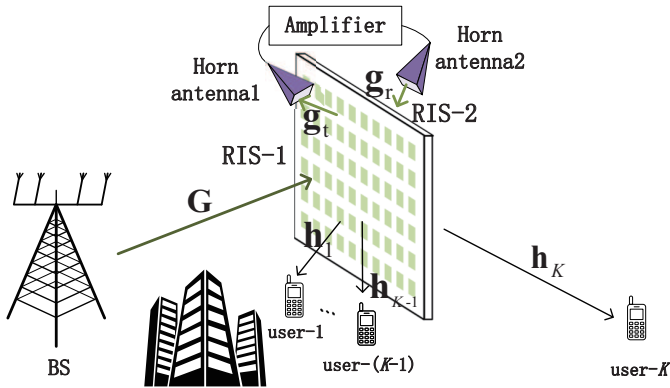


Fig. 1. The proposed reflection and relay dual-functional RIS architecture for an MU-MISO system.

far away from BS/RIS and at the back side of RIS. Based on the proposed dual-functional RIS architecture, a sum-rate maximization problem is considered for an MU-MISO system. A joint transmit beamforming and RIS reflection design algorithm is developed based on fractional programming (FP) theory and majorization-minimization (MM) technique. The convergence of the proposed algorithm is illustrated by simulation results. The performance of the proposed reflection and relay dual-functional RIS is also validated by simulations, which demonstrate the superiority of the dual-functional RIS architecture and the effectiveness of the proposed algorithm.

II. SYSTEM MODEL

We consider a reflection and relay dual-functional RIS assisted wireless communication system as illustrated in Fig. 1. The BS equipped with N antennas communicates to K single-antenna users with the aid of a dual-functional RIS. Specifically, the dual-functional RIS we proposed is composed of two conventional passive RISs connected via an amplifier. Each conventional passive RIS comprises a large number of passive elements, each being able to reflect the incident signal with a controllable phase-shift. As shown in Fig. 1, users $1, \dots, K-1$, are located around RIS and served by the side facing them (which is labelled as RIS-1 in Fig. 1). Meanwhile, the K -th user cannot receive sufficient strong signals from the BS or RIS-1 due to the fact that it is located in the opposite of the RIS-1 and the direct link to BS is blocked. Therefore, we propose a reflection and relay dual-functional RIS scheme to provide satisfactory QoS to all users, no matter they are located on either side of the RIS. In order to realize the relay functionality, the signal from the BS is first reflected by RIS-1 to horn antenna-1, then amplified and emitted to the second (right) side of the RIS (labeled as RIS-2), which transmits the signal towards the K -th user. Since two sides of the complex RIS are deployed against each other, we assume that there exists no link from RIS-1 to the K -th user nor from RIS-2 to the remaining $(K-1)$ users.

Specifically, each side of the dual-functional RIS has M passive reconfigurable elements, whose phase shifters can be adjusted by a controller. We define the reflection coefficient vector $\phi_1 \triangleq [e^{j\theta_1^1}, \dots, e^{j\theta_M^1}]^T$ and reflection matrix

$\Phi_1 \triangleq \text{diag}(\phi_1)$, with θ_m^1 denoting the phase-shift of the m -th element of RIS-1. Similarly, the notations ϕ_2 and Φ_2 are defined in the same way to represent the phase-shift of RIS-2. To be realistic, it is assumed that there is no line-of-sight (LoS) link between the transmitter and the users, due to, for example, the blockage of buildings. Since the k -th user, $k = 1, \dots, K-1$, is solely served by the reflective RIS-1, the received signal at these reflective users can be modeled as

$$y_k = \mathbf{h}_k^H \Phi_1 \mathbf{G} \sum_{i=1}^K \mathbf{w}_i s_i + n_k, \quad k = 1, \dots, K-1, \quad (1)$$

where $s_i \in \mathbb{C}$, $i = 1, \dots, K$ is transmit symbol, $\mathbb{E}\{|s_i|^2\} = 1$, $\mathbf{w}_i \in \mathbb{C}^N$ is the beamformer at the BS for the i -th user, $\mathbf{G} \in \mathbb{C}^{M \times N}$ and $\mathbf{h}_k \in \mathbb{C}^M$ denote the channels from BS to RIS-1, from RIS-1 to user- k , respectively, and $n_k \sim \mathcal{CN}(0, \sigma_k^2)$ denotes the complex additive white Gaussian noise with variance σ_k^2 at user- k . We assume that the channel state information (CSI) of all channels involved is perfectly known. The practical CSI acquisition techniques can be found in [9], [12]. Thus, the signal-to-interference-plus-noise ratio (SINR) of the k -th reflective user can be expressed as

$$\text{SINR}_k = \frac{|\mathbf{h}_k^H \Phi_1 \mathbf{G} \mathbf{w}_k|^2}{\sum_{i \neq k}^K |\mathbf{h}_k^H \Phi_1 \mathbf{G} \mathbf{w}_i|^2 + \sigma_k^2}, \quad k = 1, \dots, K-1. \quad (2)$$

Similarly, the received signal at the input of amplifier via the horn antenna-1 can be written as

$$y_r = \mathbf{g}_t^H \Phi_1 \mathbf{G} \sum_{i=1}^K \mathbf{w}_i s_i + n_0, \quad (3)$$

where $n_0 \sim \mathcal{CN}(0, \sigma_0^2)$ denotes the thermal noise with variance σ_0^2 , $\mathbf{g}_t \in \mathbb{C}^M$ denotes the channel from RIS-1 to horn antenna-1. Then, the signal y_r is amplified and transmitted by RIS-2 towards the K -th user. The received signal at the K -th user can be written as

$$\begin{aligned} y_K &= \sqrt{\beta} \mathbf{h}_K^H \Phi_2 \mathbf{g}_r \left(\mathbf{g}_t^H \Phi_1 \mathbf{G} \sum_{i=1}^K \mathbf{w}_i s_i + n_0 \right) + n_K \\ &= \sqrt{\beta} \mathbf{h}_K^H \Phi_2 \mathbf{g}_r \mathbf{g}_t^H \Phi_1 \mathbf{G} \sum_{i=1}^K \mathbf{w}_i s_i \\ &\quad + \sqrt{\beta} \mathbf{h}_K^H \Phi_2 \mathbf{g}_r n_0 + n_K, \end{aligned} \quad (4)$$

where $\mathbf{g}_r \in \mathbb{C}^M$ denotes the channel from horn antenna-2 to RIS-2 and β denotes the amplification gain which is assumed to be a constant. Considering that the RISs and the horn antennas are deployed very closely, we use near-field propagation model to describe channels \mathbf{g}_t and \mathbf{g}_r [13]-[14], whose details are omitted due to space limitations. Thus, the SINR of the K -th user can be expressed as

$$\text{SINR}_K = \frac{\beta |\mathbf{h}_K^H \Phi_2 \mathbf{g}_r \mathbf{g}_t^H \Phi_1 \mathbf{G} \mathbf{w}_K|^2}{\beta \sum_{i \neq K}^K |\mathbf{h}_K^H \Phi_2 \mathbf{g}_r \mathbf{g}_t^H \Phi_1 \mathbf{G} \mathbf{w}_i|^2 + \xi^2}, \quad (5)$$

where $\xi^2 \triangleq \beta \sigma_0^2 |\mathbf{h}_K^H \Phi_2 \mathbf{g}_r|^2 + \sigma_K^2$ denotes the power of the received noise at the K -th user.

This paper aims at maximizing the sum-rate of the MU-MISO downlink system by jointly designing the transmit

$$\begin{aligned}
g_R(\Phi_1, \Phi_2, \mathbf{w}_k, \gamma, \tau) = & \sum_{k=1}^K \log_2(1 + \gamma_k) - \sum_{k=1}^K \gamma_k + \sum_{k=1}^{K-1} \left(2\sqrt{1 + \gamma_k} \Re \{ \tau_k^* \mathbf{h}_k^H \Phi_1 \mathbf{G} \mathbf{w}_k \} - |\tau_k|^2 \sum_{i=1}^K |\mathbf{h}_k^H \Phi_1 \mathbf{G} \mathbf{w}_i|^2 - |\tau_k|^2 \sigma_k^2 \right) \\
& + 2\sqrt{\beta(1 + \gamma_K)} \Re \{ \tau_K^* \mathbf{h}_K^H \Phi_2 \mathbf{g}_r \mathbf{g}_t^H \Phi_1 \mathbf{G} \mathbf{w}_K \} - |\tau_K|^2 \beta \sum_{i=1}^K |\mathbf{h}_K^H \Phi_2 \mathbf{g}_r \mathbf{g}_t^H \Phi_1 \mathbf{G} \mathbf{w}_i|^2 - |\tau_K|^2 \xi^2
\end{aligned} \quad (6)$$

beamformers $\mathbf{w}_k, \forall k$, at the BS and the reflection matrices Φ_1, Φ_2 of the dual-functional RIS, subject to the following constraints: i) Transmit power is less than the power budget P_T at the BS, i.e., $\sum_{k=1}^K \|\mathbf{w}_k\|^2 \leq P_T$; ii) Constant amplitude of reflection coefficients, i.e. $|\phi_1(m)| = 1, |\phi_2(m)| = 1, \forall m$. Therefore, the corresponding optimization problem can be formulated as

$$(P1) \quad \max_{\Phi_1, \Phi_2, \mathbf{w}_k} \sum_{k=1}^K \log_2(1 + \text{SINR}_k) \quad (7a)$$

$$\text{s.t.} \quad \sum_{k=1}^K \|\mathbf{w}_k\|^2 \leq P_T, \quad (7b)$$

$$|\phi_1(m)| = 1, |\phi_2(m)| = 1, \forall m. \quad (7c)$$

Obviously, the optimization problem (7) is non-convex and difficult to solve due to the unit-modulus constraints and the coupling between variables. To tackle the difficulties in (7), in the following we propose an iterative beamforming and reflection design algorithm based on fractional programming (FP) theory.

III. JOINT BEAMFORMING AND REFLECTION DESIGN

In this section, we first equivalently transform the original problem into a more tractable form based on the theory of FP. With the transformed objective function, BS beamforming and RIS reflection matrices are designed iteratively.

A. FP-Based Transformation of Objective Function

The objective in (7) is a typical function of multiple fractional parameters, which is usually difficult to solve. Motivated by [15], [16] which use FP to solve this multiple-ratio problem, we attempt to equivalently transform the original problem into a more tractable form by extracting the ratio terms $\text{SINR}_k, k = 1, \dots, K$, from the logarithmic function. Based on Lagrangian dual transform [15], the optimization problem (7) is equivalent to

$$(P2) \quad \max_{\Phi_1, \Phi_2, \mathbf{w}_k, \gamma} f_R(\Phi_1, \Phi_2, \mathbf{w}_k, \gamma) \quad (8)$$

$$\text{s.t.} \quad (7b), (7c),$$

where the objective function in (8) is

$$\begin{aligned}
f_R(\Phi_1, \Phi_2, \mathbf{w}_k, \gamma) = & \sum_{k=1}^K \log_2(1 + \gamma_k) - \sum_{k=1}^K \gamma_k \\
& + \sum_{k=1}^{K-1} \frac{(1 + \gamma_k) |\mathbf{h}_k^H \Phi_1 \mathbf{G} \mathbf{w}_k|^2}{\sum_{i=1}^K |\mathbf{h}_k^H \Phi_1 \mathbf{G} \mathbf{w}_i|^2 + \sigma_k^2} \\
& + \frac{\beta(1 + \gamma_K) |\mathbf{h}_K^H \Phi_2 \mathbf{g}_r \mathbf{g}_t^H \Phi_1 \mathbf{G} \mathbf{w}_K|^2}{\beta \sum_{i=1}^K |\mathbf{h}_K^H \Phi_2 \mathbf{g}_r \mathbf{g}_t^H \Phi_1 \mathbf{G} \mathbf{w}_i|^2 + \xi^2},
\end{aligned} \quad (9)$$

and $\gamma \triangleq [\gamma_1, \dots, \gamma_K]^T$ is auxiliary variable vector. Unfortunately, optimization problem (8) is still intractable due to the complicated form of the sum of K fractional terms. Next, we apply quadratic transform [16] on the fractional term to transform it into a solvable formula by introducing another auxiliary variable vector $\tau \triangleq [\tau_1, \dots, \tau_K]^T$. Then the optimization problem (8) can be transformed into

$$(P3) \quad \max_{\Phi_1, \Phi_2, \mathbf{w}_k, \gamma, \tau} g_R(\Phi_1, \Phi_2, \mathbf{w}_k, \gamma, \tau) \quad (10)$$

$$\text{s.t.} \quad (7b), (7c),$$

where the objective function (10) is formulated as (6) presented at the top of this page.

To attack the above problem, we adopt the block coordinate ascent (BCA) methodology to alternatively update each block of variables while keep others being fixed. The sub-problems of updating of each block will be specified in detail in the following.

B. Update Auxiliary Variable Vectors

1) Update γ

When $\Phi_1, \Phi_2, \mathbf{w}_k$ and τ are held fixed, by solving $\frac{\partial g_R}{\partial \gamma_k} = 0$ for (10), the optimal γ_k^* can be found in closed form as

$$\gamma_k^* = \begin{cases} \frac{|\mathbf{h}_k^H \Phi_1 \mathbf{G} \mathbf{w}_k|^2}{\sum_{i \neq k}^K |\mathbf{h}_k^H \Phi_1 \mathbf{G} \mathbf{w}_i|^2 + \sigma_k^2}, & k = 1, \dots, K-1, \\ \frac{\beta |\mathbf{h}_K^H \Phi_2 \mathbf{g}_r \mathbf{g}_t^H \Phi_1 \mathbf{G} \mathbf{w}_K|^2}{\beta \sum_{i \neq k}^K |\mathbf{h}_K^H \Phi_2 \mathbf{g}_r \mathbf{g}_t^H \Phi_1 \mathbf{G} \mathbf{w}_i|^2 + \xi^2}, & k = K. \end{cases} \quad (11)$$

2) Update τ

Similarly, given $\Phi_1, \Phi_2, \mathbf{w}_k$ and γ , by solving $\frac{\partial g_R}{\partial \tau_k} = 0$ for (10), the auxiliary variable τ_k^* has the following optimal value

$$\tau_k^* = \begin{cases} \frac{\sqrt{1 + \gamma_k} \mathbf{h}_k^H \Phi_1 \mathbf{G} \mathbf{w}_k}{\sum_{i=1}^K |\mathbf{h}_k^H \Phi_1 \mathbf{G} \mathbf{w}_i|^2 + \sigma_k^2}, & k = 1, \dots, K-1, \\ \frac{\sqrt{\beta(1 + \gamma_K)} \mathbf{h}_K^H \Phi_2 \mathbf{g}_r \mathbf{g}_t^H \Phi_1 \mathbf{G} \mathbf{w}_K}{\beta \sum_{i=1}^K |\mathbf{h}_K^H \Phi_2 \mathbf{g}_r \mathbf{g}_t^H \Phi_1 \mathbf{G} \mathbf{w}_i|^2 + \xi^2}, & k = K. \end{cases} \quad (12)$$

C. Update BS Beamforming

With other variables being fixed, the update of beamforming \mathbf{w}_k reduces to solving the following problem

$$(P4) \quad \max_{\mathbf{w}_k} g_R(\Phi_1, \Phi_2, \mathbf{w}_k, \gamma, \tau) \quad (13a)$$

$$\text{s.t.} \quad \sum_{k=1}^K \|\mathbf{w}_k\|^2 \leq P_T, \quad (13b)$$

which is a convex problem. Fortunately, the optimal solution of problem (13) can be obtained in an analytic form via checking

its optimality conditions. By introducing a multiplier μ for the power constraint in (13b), we can form a Lagrangian function as

$$\mathcal{L} = g_R(\Phi_1, \Phi_2, \mathbf{w}_k, \gamma, \boldsymbol{\tau}) + \mu \left(P_T - \sum_{k=1}^K \|\mathbf{w}_k\|^2 \right). \quad (14)$$

Then, the optimal solution of BS beamforming \mathbf{w}_k can be determined by setting the partial derivative of \mathcal{L} with respect to \mathbf{w}_k and μ to zero, i.e.

$$\begin{cases} \frac{\partial \mathcal{L}}{\partial \mathbf{w}_k} = 0, & \forall k, \\ \frac{\partial \mathcal{L}}{\partial \mu} = 0, \end{cases} \quad (15)$$

which yields the optimal BS beamforming as

$$\mathbf{w}_k^* = (\mathbf{A} + \mu^* \mathbf{I})^{-1} \sqrt{1 + \gamma_k} \tilde{\mathbf{h}}_k, \quad \forall k, \quad (16)$$

with

$$\tilde{\mathbf{h}}_k^H \triangleq \begin{cases} \tau_k^* \mathbf{h}_k^H \Phi_1 \mathbf{G}, & k = 1, \dots, K-1, \\ \sqrt{\beta} \tau_k^* \mathbf{h}_k^H \Phi_2 \mathbf{g}_t \mathbf{g}_t^H \Phi_1 \mathbf{G}, & k = K, \end{cases} \quad (17)$$

$$\mathbf{A} \triangleq \sum_{k=1}^K \tilde{\mathbf{h}}_k \tilde{\mathbf{h}}_k^H, \quad (18)$$

where the optimal multiplier μ^* can be easily obtained by a bisection search.

D. Update RIS Reflection

Given γ , $\boldsymbol{\tau}$ and BS beamforming $\mathbf{w}_k, \forall k$, the sub-problem with respect to the RIS reflection matrices Φ_1 and Φ_2 can be presented as:

$$(P5) \quad \max_{\Phi_1, \Phi_2} g_R(\Phi_1, \Phi_2, \mathbf{w}_k, \gamma, \boldsymbol{\tau}) \quad (19a)$$

$$\text{s.t.} \quad |\phi_1(m)| = 1, \quad |\phi_2(m)| = 1, \quad \forall m. \quad (19b)$$

Considering that Φ_1 and Φ_2 are coupled and jointly yield a nonconvex objective, we turn to separately optimize either of them with the other being fixed. When Φ_2 is given, by defining

$$\mathbf{r}_{k,i}^H \triangleq \begin{cases} \tau_k^* \mathbf{h}_k^H \text{diag}(\mathbf{G} \mathbf{w}_i), & k = 1, \dots, K-1, \forall i, \\ \sqrt{\beta} \tau_k^* \mathbf{h}_k^H \Phi_2 \mathbf{g}_t \mathbf{g}_t^H \text{diag}(\mathbf{G} \mathbf{w}_i), & k = K, \forall i, \end{cases} \quad (20)$$

$$\tilde{\mathbf{R}} \triangleq \sum_{k=1}^K \sum_{i=1}^K \mathbf{r}_{k,i} \mathbf{r}_{k,i}^H, \quad (21)$$

$$\mathbf{d} \triangleq \sum_{k=1}^K \sqrt{(1 + \gamma_k)} \mathbf{r}_{k,k}, \quad (22)$$

and removing constants, the optimization of Φ_1 (19) is equivalent to solving the following problem

$$(P6) \quad \min_{\phi_1} - \sum_{k=1}^K \left(2\sqrt{1 + \gamma_k} \Re \{ \mathbf{r}_{k,k}^H \phi_1 \} - \sum_{i=1}^K |\mathbf{r}_{k,i}^H \phi_1|^2 \right)$$

$$= \phi_1^H \tilde{\mathbf{R}} \phi_1 - 2\Re \{ \phi_1^H \mathbf{d} \} \quad (23a)$$

$$\text{s.t.} \quad |\phi_1(m)| = 1, \quad m = 1, \dots, M. \quad (23b)$$

Problem (23) is still difficult to solve due to the constant modulus constraint. To effectively solve this problem, we adopt

the majorization-minimization (MM) algorithm to perform the updating more easily. The central idea of MM framework is to sequentially surrogate the original objective function with a tightly upper-bounded approximation, which is designed to render the transformed problem more tractable [17]. Given the update value ϕ_1^t in the previous iteration, we propose to majorize the objective function of problem (23) via executing its second-order Taylor expansion at the point of ϕ_1^t followed by replacing the associated quadratic term with an upper bound. Specifically, the quadratic term in (23) is majorized by

$$\begin{aligned} \phi_1^H \tilde{\mathbf{R}} \phi_1 &\leq \phi_1^H \boldsymbol{\Lambda} \phi_1 - 2\Re \left\{ \phi_1^H (\boldsymbol{\Lambda} - \tilde{\mathbf{R}}) \phi_1^t \right\} \\ &\quad + (\phi_1^t)^H (\boldsymbol{\Lambda} - \tilde{\mathbf{R}}) \phi_1^t, \end{aligned} \quad (24)$$

where $\boldsymbol{\Lambda} \triangleq \lambda_{\max} \mathbf{I}_M$ and λ_{\max} is the maximum eigenvalue of $\tilde{\mathbf{R}}$. Then, the subproblem to be solved at the $(t+1)$ -th iteration is given by

$$\min_{\phi_1} \phi_1^H \boldsymbol{\Lambda} \phi_1 - 2\Re \left\{ \phi_1^H (\boldsymbol{\Lambda} - \tilde{\mathbf{R}}) \phi_1^t \right\} \quad (25a)$$

$$+ (\phi_1^t)^H (\boldsymbol{\Lambda} - \tilde{\mathbf{R}}) \phi_1^t - 2\Re \{ \phi_1^H \mathbf{d} \} \quad (25b)$$

$$\text{s.t.} \quad |\phi_1(m)| = 1, \quad m = 1, \dots, M. \quad (25c)$$

Since $\phi_1^H \phi_1 = M$, we have $\phi_1^H \boldsymbol{\Lambda} \phi_1 = M \lambda_{\max}$, which is a constant. By removing the constants, problem (25) can be rewritten as follows

$$\max_{\phi_1} 2\Re \{ \phi_1^H \mathbf{p}^t \} \quad (26a)$$

$$\text{s.t.} \quad |\phi_1(m)| = 1, \quad m = 1, \dots, M, \quad (26b)$$

where $\mathbf{p}^t \triangleq (\lambda_{\max} \mathbf{I}_M - \tilde{\mathbf{R}}) \phi_1^t + \mathbf{d}$. Thus, the optimal solution of problem (26) is given by

$$\phi_1^{t+1} = e^{j \arg(\mathbf{p}^t)}. \quad (27)$$

If low-resolution phase shifters are employed to realize the RIS, the corresponding reflection coefficient can be obtained using a simple quantization operation, i.e.

$$\tilde{\phi}_1^{t+1} = \exp \left\{ j \left\langle \frac{\arg(\mathbf{p}^t)}{\Delta} \right\rangle \times \Delta \right\}, \quad (28)$$

where $\langle \cdot \rangle$ denotes the rounding operation, and $\Delta \triangleq 2\pi/2^b$ is the angle resolution controlled by b bits.

After obtaining ϕ_1 , we can similarly solve ϕ_2 by just repeating the same procedure. Specifically, by defining

$$\mathbf{v}_{K,k}^H \triangleq \sqrt{\beta} \tau_k^* \mathbf{h}_k^H \text{diag}(\mathbf{g}_t \mathbf{g}_t^H \Phi_1 \mathbf{G} \mathbf{w}_k), \quad \forall k, \quad (29)$$

$$\tilde{\mathbf{V}} \triangleq \sum_{k=1}^K \mathbf{v}_{K,k} \mathbf{v}_{K,k}^H, \quad (30)$$

$$\mathbf{b} \triangleq \sqrt{(1 + \gamma_K)} \mathbf{v}_{K,K}, \quad (31)$$

and removing the other constant terms unrelated to ϕ_2 , problem (19) can be rearranged as

$$(P7) \quad \min_{\phi_2} - 2\sqrt{(1 + \gamma_K)} \Re \{ \mathbf{v}_{K,K}^H \phi_2 \} + \sum_{i=1}^K |\mathbf{v}_{K,i}^H \phi_2|^2$$

$$= \phi_2^H \tilde{\mathbf{V}} \phi_2 - 2\Re \{ \phi_2^H \mathbf{b} \} \quad (32a)$$

Algorithm 1 Joint Beamforming and RIS Reflection Design

Input: $\mathbf{h}_k, \forall k, \mathbf{G}, \mathbf{g}_r, \mathbf{g}_t, b, \sigma^2, \sigma_0^2, \beta, P_T, T_{max}$.

Output: $\mathbf{w}_k^*, \forall k, \Phi_1^*, \Phi_2^*$.

- 1: Initialize $\mathbf{w}_k, \forall k, \Phi_1, \Phi_2$.
- 2: **Repeat**
- 3: Update γ^* by (11).
- 4: Update τ^* by (12).
- 5: Update each beamforming vector $\mathbf{w}_k^*, \forall k$, by solving (16).
- 6: Set $t = 1$.
- 7: **while** $t < T_{max}$ & no convergence of Φ_1 do
- 8: Update ϕ_1^{t+1} by (27)/(28).
- 9: $t := t + 1$.
- 10: **end while**
- 11: Set $t = 1$.
- 12: **while** $t < T_{max}$ & no convergence of Φ_2 do
- 13: Update ϕ_2^{t+1} by (33)/(34).
- 14: $t := t + 1$.
- 15: **end while**
- 16: **Until convergence**
- 17: Return $\mathbf{w}_k^*, \forall k, \Phi_1^*, \Phi_2^*$.

$$\text{s.t. } |\phi_2(m)| = 1, m = 1, \dots, M. \quad (32b)$$

Following the identical argument as before, the optimal solution of problem (32) is given by

$$\phi_2^{t+1} = e^{j \arg(\mathbf{q}^t)}. \quad (33)$$

where $\mathbf{q}^t \triangleq (\zeta_{\max} \mathbf{I}_M - \tilde{\mathbf{V}}) \phi_2^t + \mathbf{b}$ and ζ_{\max} is the maximum eigenvalue of $\tilde{\mathbf{V}}$.

If low-resolution phase shifters are employed, the corresponding reflection coefficient can be obtained using the quantization operation, i.e.

$$\tilde{\phi}_2^{t+1} = \exp \left\{ j \left\langle \frac{\arg(\mathbf{q}^t)}{\Delta} \right\rangle \times \Delta \right\}. \quad (34)$$

Now, the complete procedure of finding the optimal auxiliary vectors γ^* and τ^* , the BS beamforming \mathbf{w}_k^* , and RIS reflection matrices Φ_1^*, Φ_2^* is straightforward. With appropriate initialization, we iteratively update $\gamma, \tau, \mathbf{w}_k$ and Φ_1, Φ_2 until convergence. For clarity, the proposed FP-based BS beamforming and RIS reflection design algorithm is summarized in Algorithm 1.

IV. SIMULATION RESULTS

In this section, we provide simulation results to demonstrate the advantages of the proposed dual-functional RIS architecture and illustrate the effectiveness of our proposed algorithm. The noise power at all receivers is $\sigma_k^2 = -80\text{dBm}$ and the thermal noise power introduced by the amplifier is $\sigma_0^2 = -70\text{dBm}$ [1]. The path-loss is modeled as $\text{PL}(d) = C_0 (d_0/d)^\kappa$, where $C_0 = -30\text{dB}$, $d_0 = 1\text{m}$, d is the link distance, and κ is the path-loss exponent. The BS-RIS channel is assumed to follow a small-scale Rician fading model with a Rician factor of 3dB and a path-loss exponent of 2.5, while the other channels only have non-line-of-sight (NLoS) components and a path-loss exponent of 3. The channel \mathbf{g}_t from RIS-1 to horn antenna and the channel \mathbf{g}_r from horn antenna to RIS-2 adopt near-field model [13], [14]. The BS is equipped with $N = 6$ antennas and serves $K = 4$ users. The RIS is 50m away from the BS,

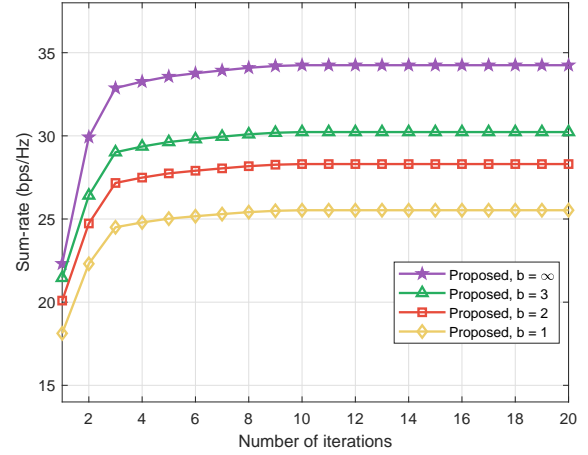


Fig. 2. Sum-rate versus the number of iterations ($P_T = 40\text{dBm}$, $M = 64$).

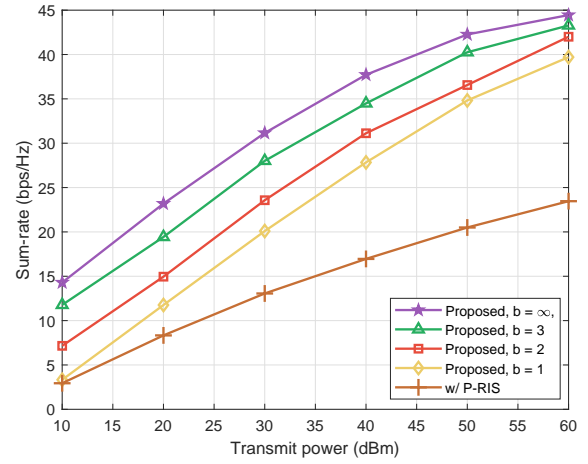


Fig. 3. Sum-rate versus the transmit power P_T ($M = 64$, $\beta = 30\text{dB}$).

while the three users ($k = 1, 2, 3$) are 2m away from the dual-functional RIS and the fourth user ($k = 4$) is 20m away from the RIS.

We start with presenting the convergence of the proposed joint BS beamforming and RIS reflection design by plotting the sum-rate versus the number of iterations in Fig. 2. Simulation result illustrates that the proposed algorithm can converge within 15 iterations when using continuous ($b = \infty$) phase shifters to realize the RIS. For the case of employing low-resolution ($b = 1, 2, 3$ bit) phase shifters, the proposed algorithm will converge faster within 10 iterations.

Next, Fig. 3 shows the achievable sum-rate versus transmit power P_T for the case that RIS uses continuous and $b = 1, 2, 3$ -bit resolution phase shifters. It can be observed that the proposed dual-functional RIS architecture can achieve satisfactory performance. For comparison, we also include the case that only one passive RIS (w/ P-RIS) is deployed as the benchmark. We can notice that the proposed dual-functional RIS can substantially enhance the communication

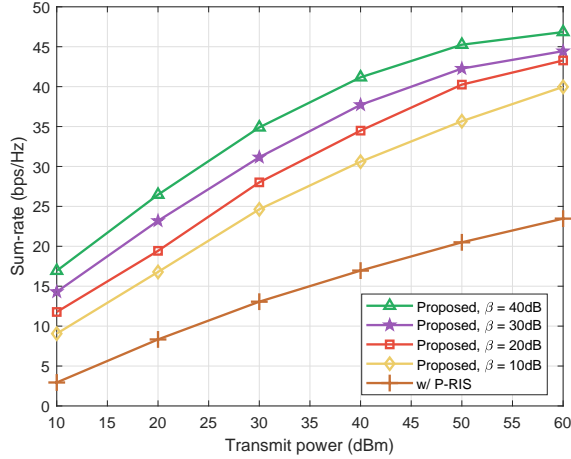


Fig. 4. Sum-rate versus the transmit power P_T for different amplifier gain β ($M = 64$, $b = \infty$).

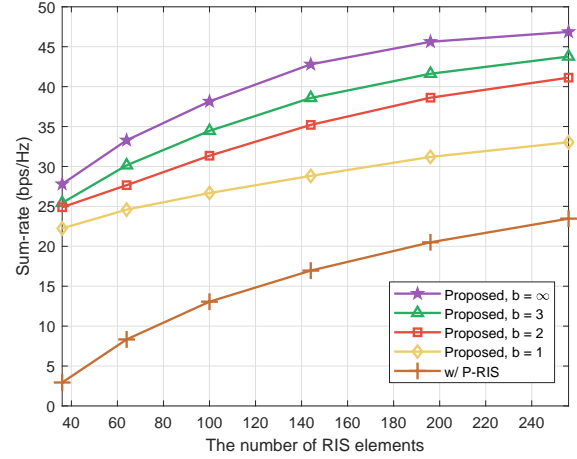


Fig. 5. Sum-rate versus the number of RIS elements M ($P_T = 40\text{dBm}$, $\beta = 30\text{dB}$).

quality compared with the case that the conventional passive RIS is deployed, which indicates the effectiveness of deploying dual-functional RIS.

Fig. 4 shows the sum-rate with the proposed dual-functional RIS architecture under different realistic values for the amplification gain β . It is noted that the dual-functional RIS with a reasonable amplification gain can result in better performance compared with only one passive RIS. When the amplification gain β is 40dB, only 30dBm transmit power is need to achieve the same performance, for example, sum-rate is around 35 bps/Hz, while 50dBm transmit power is need as amplification gain β is 10dB.

In Fig. 5, the sum-rate versus the numbers of RIS elements M is plotted. The same conclusion can be drawn that the proposed architecture can always achieve satisfactory performance, which illustrates the advantages of employing the dual-functional RIS in wireless communication systems. As we can see, only 36 elements with RIS adopting 1-bit resolution phase shifters in proposed dual-functional RIS are needed to achieve the same performance as 256 elements are needed when conventional passive RIS is implemented.

V. CONCLUSIONS

In this paper, we introduced a novel reflection and relay dual-functional RIS architecture to overcome the double fading effect and enhance the coverage of downlink MU-MISO system. Aiming at maximizing the achievable sum-rate, an iterative algorithm based on FP and MM was proposed to design the transmit beamforming and RIS reflection. Simulation results demonstrated the superiority of the introduced dual-functional RIS architecture and the effectiveness of the proposed algorithm.

REFERENCES

- [1] Q. Wu and R. Zhang, "Towards smart and reconfigurable environment: Intelligent reflecting surface aided wireless network," *IEEE Commun. Mag.*, vol. 58, no. 1, pp. 106-112, Jan. 2020.
- [2] E. Basar, M. D. Renzo, J. D. Rosny, M. Debbah, M. Alouini, and R. Zhang, "Wireless communications through reconfigurable intelligent surfaces," *IEEE Access*, vol. 7, pp. 116753-116773, Sep. 2019.

- [3] S. Hu, F. Rusek, and O. Edfors, "Beyond massive MIMO: The potential of positioning with large intelligent surfaces," *IEEE Trans. Signal Process.*, vol. 66, no. 7, pp. 1761-1774, Apr. 2018.
- [4] M. D. Renzo, et al., "Smart radio environments empowered by reconfigurable AI meta-surfaces: An idea whose time has come," *EURASIP J. Wireless Commun. Netw.*, vol. 19, no. 1, pp. 1-20, Dec. 2019.
- [5] M. Najafi, V. Jamali, R. Schober, and H. Vincent Poor, "Physicsbased modeling and scalable optimization of large intelligent reflecting surfaces," *IEEE Trans. Commun.*, vol. 69, no. 4, pp. 2673-2691, Dec. 2020.
- [6] Z. Zhang, L. Dai, X. Chen, C. Liu, F. Yang, R. Schober, and H. V. Poor, "Active RIS vs. passive RIS: Which will prevail in 6G?" Mar. 2021. [Online]. Available: <https://arxiv.org/abs/2103.15154>
- [7] E. Björnson, Ö. Özdogan, and E. G. Larsson, "Intelligent reflecting surface versus decode-and-forward: How large surfaces are needed to beat relaying?" *IEEE Wireless Commun. Lett.*, vol. 9, no. 2, pp. 244-248, Oct. 2020.
- [8] K. Ntontin, M. D. Renzo, and F. Lazarakis, "On the rate and energy efficiency comparison of reconfigurable intelligent surfaces with relays," in *Proc. IEEE Conf. Signal Process. Advances Wireless Commun. (SPAWC Workshop)*, Atlanta, USA, May 2020, pp. 1-5.
- [9] C. You, B. Zheng, and R. Zhang, "Channel estimation and passive beamforming for intelligent reflecting surface: Discrete phase shift and progressive refinement," *J. Sel. Areas Commun.*, vol. 38, no. 11, pp. 2604-2620, Nov. 2020.
- [10] X. Ying, U. Demirhan, and A. Alkhateeb, "Relay aided intelligent reconfigurable surfaces: Achieving the potential without so many antennas," Jun. 2020. [Online]. Available: <https://arxiv.org/abs/2006.06644>
- [11] N. T. Nguyen, Q.-D. Vu, K. Lee, and M. Juntti, "Hybrid relay-reflecting intelligent surface-assisted wireless communication," Mar. 2021. [Online]. Available: <https://arxiv.org/abs/2103.03900>
- [12] Z. Wang, L. Liu, and S. Cui, "Channel estimation for intelligent reflecting surface assisted multiuser communications: Framework, algorithms, and analysis," *IEEE Trans. Wireless Commun.*, vol. 19, no. 10, pp. 6607-6620, Oct. 2019.
- [13] X. Cheng and Y. He, "Channel modeling and analysis of ULA massive MIMO systems," in *Proc. Int. Conf. Advanced Commun. Tech. (ICACT)*, Gangwon-do, South Korea, Feb. 2018, pp. 411-416.
- [14] E. Björnson and L. Sanguinetti, "Power scaling laws and near-field behaviors of massive MIMO and intelligent reflecting surfaces," *IEEE Open J. Commun. Society*, vol. 1, pp.1306-1324, Sep. 2020.
- [15] K. Shen and W. Yu, "Fractional programming for communication systems-Part I: Power control and beamforming," *IEEE Trans. Signal Process.*, vol. 66, no. 10, pp. 2616-2630, May 2018.
- [16] K. Shen and W. Yu, "Fractional programming for communication systems-Part II: Uplink scheduling via matching," *IEEE Trans. Signal Process.*, vol. 66, no. 10, pp. 2631-2644, May 2018.
- [17] Y. Liu and J. Li, "Linear precoding to optimize throughput, power consumption and energy efficiency in MIMO wireless sensor networks," *IEEE Trans. Commun.*, vol. 66, no. 5, pp. 2122-2136, May 2018.

This figure "0512con.png" is available in "png" format from:

<http://arxiv.org/ps/2107.11579v1>

This figure "0514beta.png" is available in "png" format from:

<http://arxiv.org/ps/2107.11579v1>

This figure "0514num.jpg" is available in "jpg" format from:

<http://arxiv.org/ps/2107.11579v1>

This figure "0514num.png" is available in "png" format from:

<http://arxiv.org/ps/2107.11579v1>

This figure "0514power.png" is available in "png" format from:

<http://arxiv.org/ps/2107.11579v1>

This figure "system.png" is available in "png" format from:

<http://arxiv.org/ps/2107.11579v1>